Comparison between Phase Shift and Complex Potential Descriptions of Elastic Scattering*

JONAS ALSTER
Physics Department, University of Washington, Seattle, Washington†
and
Lawrence Radiation Laboratory, University of California, Berkeley, California

AND

HOMER E. CONZETT
Lawrence Radiation Laboratory, University of California, Berkeley, California

(Received 17 February 1965)

The equivalence between parametrized phase-shift and complex-potential analyses of the elastic scattering of strongly absorbed particles is discussed. Specific comparisons are made using computer analyses of alpha-particle scattering data. The relative merits of the two analyses are pointed out.

I. INTRODUCTION

IN this paper we want to emphasize the equivalence between parametrized phase-shift (PPS) and complex-potential model (CPM) analyses of the elastic scattering of strongly absorbed[1] "particles," such as He^3, alpha-particles, deuterons, and heavier ions. We make specific comparisons using analyses of alpha-particle scattering data. Then we point out several advantages of the PPS method, which encompasses all analyses[2–7] in which the partial-wave (complex) phase shifts are explicitly parametrized in the calculation and are not adjusted through an intermediary complex potential.

The differential cross secrion for elastic scattering is

$$\sigma(\theta)=|f(\theta)|^2,$$

with the scattering amplitude, in the absence of spin-dependent interactions, given by

$$f(\theta)=f_c(\theta)+(i/2k)\sum_{l=0}^{\infty}(2l+1)e^{2i\sigma_l}(1-\eta_l)P_l(\cos\theta)\,, \quad (1)$$

where $f_c(\theta)$ is the Coulomb scattering amplitude, $k=(1/\hbar)(2\mu E)^{1/2}$, $\sigma_l=\arg\Gamma(1+l+in)$, with $n=z_1z_2e^2/\hbar v$. One can write

$$\eta_l=A_le^{2i\delta_l} \quad (2)$$

so that A_l, the amplitude of the *outgoing* lth partial wave, and δ_l, its nuclear phase shift, are real. Thus, $0\leq A_l\leq 1$, with $A_l=1$ corresponding to no absorption and $A_l=0$, to complete absorption of that partial wave. McIntyre *et al.*[2] introduced the (arbitrary) parameterization

$$A_l=1-\left[1+\exp\frac{l-l_A}{\Delta l_A}\right]^{-1}, \quad \delta_l=\delta\left[1+\exp\frac{l-l_\delta}{\Delta l_\delta}\right]^{-1} \quad (3)$$

as an improvement over the "sharp cutoff" model (see Fig. 1). This form for A_l has been justified by Elton,[5] whereas a form of δ_l suggested by Conzett *et al.*[3] as having qualitative theoretical justification, differs from that of Eq. (3), particularly for $l<l_\delta$. However, we shall see, for those cases examined here, that the scattering amplitude is not seriously affected because in the region of l values for which Eq. (3) is incorrect, $A_l\to 0$. This would not be the case for less strongly absorbed particles, and thus a theoretically proper form of δ_l would be required.

* This paper is based on a thesis submitted to the Technical University of Delft, The Netherlands, in partial fulfillment of the Ph.D. degree; University of California Lawrence Radiation Laboratory report UCRL-9650, 1961 (unpublished). This work was done under the auspices of the U. S. Atomic Energy Commission.

† Present address: Physics Department, University of Washington, Seattle, Washington.

[1] As used here, absorption encompasses all transitions out of the entrance channel.

[2] For alpha-particle scattering: J. S. Blair, Phys. Rev. **95**, 1218 (1954), "sharp cutoff" model; J. A. McIntyre, K. H. Wang, and L. C. Becker, Phys. Rev. **117**, 1337 (1960), modified "sharp cutoff" model.

[3] For heavy-ion scattering: J. Alster and H. E. Conzett, *Proceedings of the Second Conference on Reactions between Complex Nuclei*, edited by A. Zucker, E. C. Halbert, and F. T. Howard (John Wiley & Sons, Inc., New York, 1960), p. 175; J. Alster, thesis, University of California, Lawrence Radiation Laboratory Report UCRL-9650, 1961 (unpublished); J. A. McIntyre, S. D. Baker, and K. H. Wang, Phys. Rev. **125**, 584 (1962); H. E. Conzett, A. Isoya, and E. Hadjimichael, *Proceedings of the Third Conference on Reactions between Complex Nuclei*, edited by A. Ghiorso, R. M. Diamond, and H. E. Conzett (University of California Press, Berkeley, 1963).

[4] G. Igo, Phys. Rev. **115**, 1665 (1959); H. E. Conzett, A. Isoya and E. Hadjimichael, Ref. 3. Detailed investigations pertinent to this point have been made by G. H. Rawitscher, J. S. McIntosh, and J. A. Polak, *Proceedings of the Third Conference on Reactions between Complex Nuclei*, edited by A. Ghiorso, R. M. Diamond, and H. E. Conzett (University of California Press, Berkeley, 1963); R. M. Drisko, G. R. Satchler, and R. H. Bassel, Phys. Letters **5**, 347 (1963); J. S. McIntosh, S. C. Park, and G. H. Rawitscher, Phys. Rev. **134**, B1010 (1964); G. H.Rawitscher,*ibid.* **135**, B605 (1964).

[5] J. Alster and H. E. Conzett, Phys. Rev. **136**, B1024 (1964).

[6] Applications to high-energy nucleon scattering have been developed by K. R. Greider and A. E. Glassgold, Ann. Phys. (N.Y.) **10**, 100 (1960); and L. R. B. Elton, Nucl. Phys. **23**, 681 (1961).

[7] For a very complete analytical development of PPS analyses of elastic scattering of strongly absorbed particles see W. E. Frahn and R. H. Venter, Ann. Phys. (N. Y.) **24**, 243 (1963); R. H. Venter, *ibid.* **25**, 405 (1963).

The CPM analysis determines A_l and δ_l by solving the equation satisfied by the radial wave function, $f_l(r)$:

$$\left[\frac{d^2}{dr^2}-\frac{l(l+1)}{r^2}+k^2-\frac{2\mu}{\hbar^2}U(r)\right]f_l(r)=0, \quad (4)$$

where $U(r)=V_c(r)+V_N(r)$, the Coulomb plus the nuclear potential. In order to provide a description of both the elastic scattering and absorptive processes, the latter is taken to be complex: $V_N(r)=-[V(r)+iW(r)]$. Comparison at $r=\infty$ of $f_l(r)$ with the solution of Eq. (4) for $V_N(r)=0$ then gives A_l and δ_l. Strongly absorbed particles sample only the surface region of the nucleus, so one is justified in questioning the significance of using a parametrized complex potential to describe the scattering.[4] The PPS analysis parameterizes the A_l and δ_l directly, so it is clear that the two analyses can be equivalent.

II. COMPARISON OF THE ANALYSES

For purposes of comparison, one can make the correspondence between l and r, the distance of closest approach for a particle of orbital angular momentum $[l(l+1)]^{1/2}\hbar$, through the relation

$$kr=n+[n^2+l(l+1)]^{1/2}. \quad (5)$$

We indicate this correspondence between coordinate (r) space and orbital angular-momentum (l) space by writing $A_l(r)$. The value of $r=R_a$ for which $A_l(r)=\frac{1}{2}$ should not be expected to agree with the value of $r=R$ for which $V(R)=\frac{1}{2}V(0)$ in the CPM. Similarly, t, the interval Δl_A converted to coordinate space via Eq. (5), would not necessarily agree with the analogous complex-potential surface-thickness parameter a. These points have been developed previously.[5]

In order to demonstrate these considerations more explicitly, we have made PPS analyses of some existing

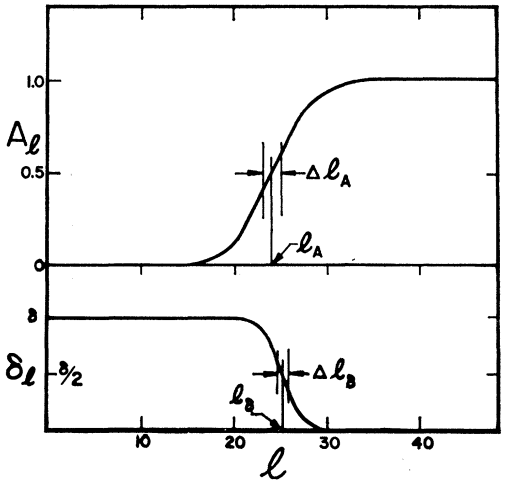

FIG. 1. A_l is the amplitude of the outgoing lth partial wave, and δ_l is its nuclear phase shift.

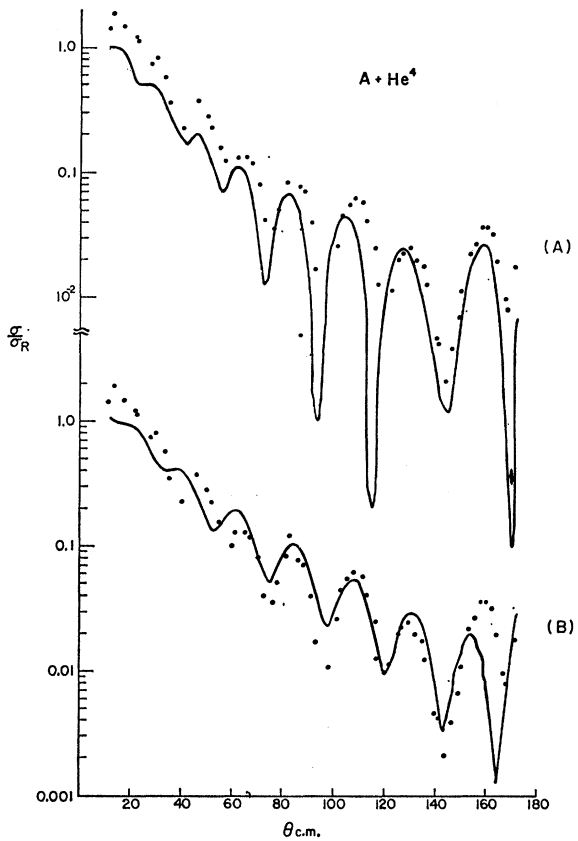

FIG. 2. (A) The solid line is the CPM fit to the elastic scattering of He^4 from Ar (reference 10). Parameters are: $V=100$ MeV, $W=-15$ MeV; $R=(1.17A^{1/3}+1.36)$ F, $a=0.6$ F. (B) The solid line gives the PPS fit to the same data with the parameters $l_A=7.5$, $\Delta l_A=0.6$, $\delta=1.2$, $l_\delta=6.5$, $\Delta l_\delta=0.5$. The points give the experimental values.

data on the elastic scattering of alpha particles from Ar, Cu, and Pb at 18, 40, and 48 MeV, respectively.[8–10] These data had previously been used for a CPM analysis.[11] Figures 2–4 show comparisons between experimental and calculated angular distributions for both PPS and CPM analyses. In all cases the quality of agreement between experiment and calculation is comparable for the two treatments; in some cases one analysis gives better agreement than the other, depending to some extent on what feature of the data is regarded as most significant. The values of the parameters resulting from these analyses are compiled in Table I, together with those resulting from PPS[2] and CPM[12] analyses of data on the scattering of 22 and 40-MeV alpha particles from Ag. The expected differences between the com-

[8] L. Seidlitz, E. Bleuler, and D. J. Tendam, Phys. Rev. **110**, 682 (1958).
[9] G. Igo, H. E. Wegner, and R. M. Eisberg, Phys. Rev. **101**, 1508 (1956).
[10] R. E. Ellis and L. Schecter, Phys. Rev. **101**, 636 (1956).
[11] G. Igo, Phys. Rev. **115**, 1665 (1959).
[12] W. B. Cheston and A. E. Glassgold, Phys. Rev. **106**, 1215 (1957); A. E. Glassgold, Progr. Nucl. Phys. **7**, 123 (1959).

TABLE I. Comparison of parameters resulting from PPS and CPM analyses of alpha-particle scattering data.

Data		CPM analysis parameters						PPS analysis			
	E_α (MeV)	V (MeV)	W (MeV)	R (F)	a (F)	l_A	Δl_A	l_A	Δl_A	R_a	t
Ar+He^4	18	100	15	5.4	0.6	*9.7*[a]	*0.6*	*7.5*[a]	*0.6*	6.67	0.33
Cu+He^4	40	49.3	11	6.8	0.5	*17.8*	*0.8*	*17.0*	*0.8*	7.92	0.30
Pb+He^4	48	25	15	8.1	0.6	*21.1*	*1.3*	*21.0*	*1.3*	10.16	0.41
Ag+He^4 [b]	22	50	20	7.5	0.6	*10.5*	*1.5*	*10.8*	*0.75*[c]	9.74	0.33
		150	20	7.5	0.6	*11.3*	*1.3*	*10.8*	*0.75*	9.74	0.33
Ag+He^4 [b]	40	50	20	7.1	0.6	*19.3*	*1.2*	*19.0*	*1.1*	9.27	0.40
		150	20	7.1	0.6	*19.8*	*1.1*	*19.0*	*1.1*	9.27	0.40

[a] The disagreement in l_A values in this case arises from the difference in fits to the experimental data.
[b] From Refs. 2 (McIntyre *et al.*) and 12.
[c] This Δl_A value resulted from an analysis in which δ_l was zero. This may account for its being appreciably lower than the value determined from the CPM analysis.

plex-potential parameters, R and a, and the PPS parameters, R_a and t, are seen. If one now looks at the actual scattering amplitude parameters describing the l-dependence A_l and δ_l, the equivalence of the two analyses is seen. That is, the l_A and Δl_A values determined from the separate analyses are in excellent agree-

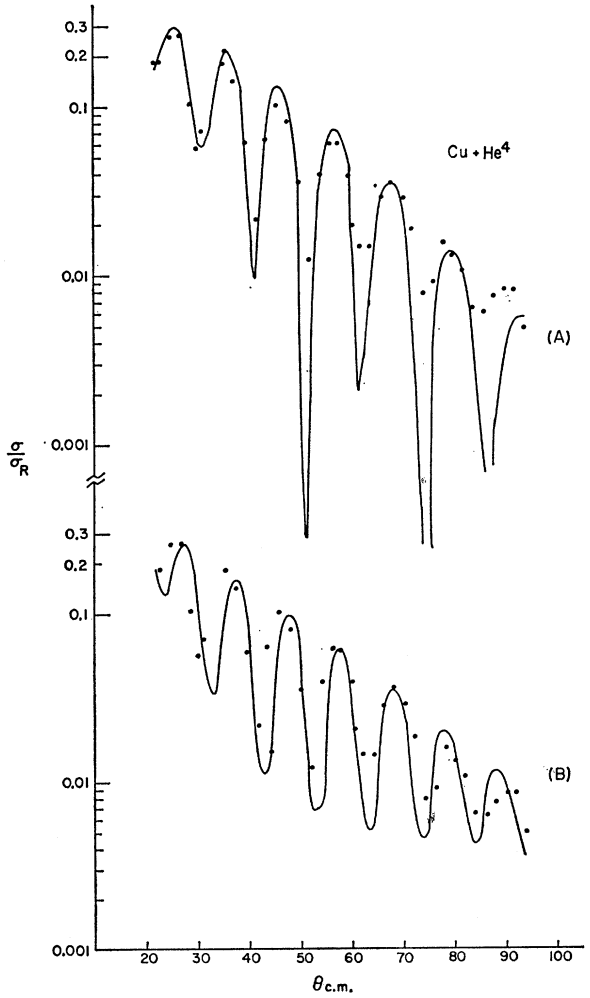

FIG. 3. (A) Same as 2(A) for He^4 scattered from Cu (Ref. 10). The parameters are $V=-49.3$ MeV, $W_0=-11$ MeV, $R=(1.14A^{1/3}+2.24)$ F, $a=0.5$ F. (B) Same as 2(B). The parameters are: $l_A=17$, $\Delta l_A=0.8$, $\delta=0.7$, $l_\delta=17$, $\Delta l_\delta=1.0$.

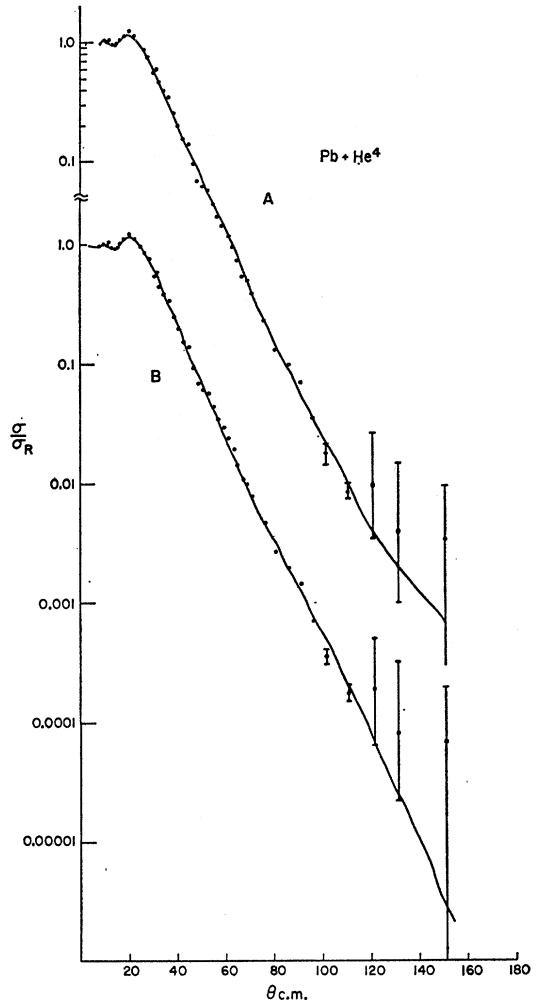

FIG. 4. (A) Same as 2(A) for He^4 scattered from Pb (Ref. 10). The parameters are $V=-25$ MeV, $W=-15$ MeV, $R=(1.13A^{1/3}+2.0)$ F, $a=0.6$ F. (B) Same as 2(B). The parameters are: $l_A=21$, $\Delta l_A=1.3$, $\delta=0.2$, $l_\delta=23$, $\Delta l_\delta=1.4$.

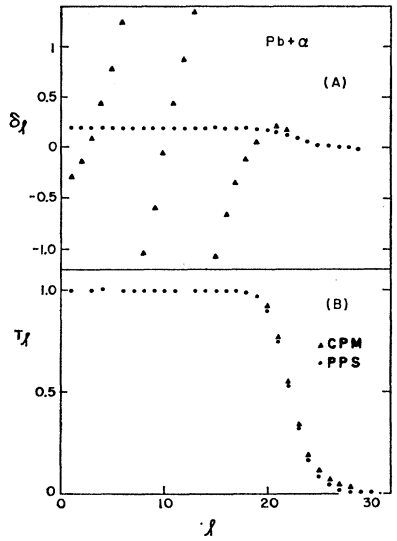

FIG. 5. (A) Plot of δ_l as a function l for the CPM (•) and PPS (Δ) analyses of the Pb+He⁴ elastic scattering data. (B) Plot of $T_l=1-A_l^2$ as a function of l for the CPM (•) and PPS (Δ) analyses.

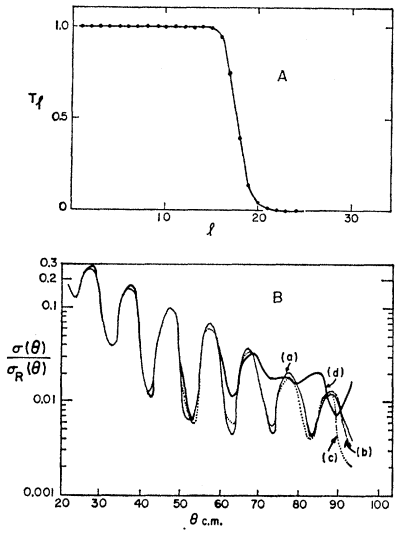

FIG. 6. (A) The factor T_l is plotted as a function of l for PPS analysis of the Cu+He⁴ scattering data. (B) Curve a gives the ratio to Rutherford scattering calculated with the PPS parameters: $l_A=17$, $\Delta l_A=0.8$, $\delta=0.7$, $l_\delta=17$, $\Delta l_\delta=1.0$. Curve b gives the same calculation, making $\delta_l=0$ for $l<14$. Curve c gives the same calculation, making $\delta_l=0$ for $l<15$. Curve d gives the same calculation, making $\delta_l=0$ for $l<16$.

ment, and the differences in the coordinate parameters, R_0 and a versus R_a and t, clearly result from their different physical definition. As a further specific illustration, we show in Fig. 5 the l-space dependence of δ_l and $T_l=1-A_l^2(=\sigma_l^r/(2l+1)\pi\lambda\!\!\!^{-2}$, where σ_l^r is the lth-wave partial-reaction cross section) resulting from the two analyses of the Pb scattering data. As remarked above, the large differences between the PPS and CPM values of δ_l for $l\leq 18$ do not result in noticeably different scattering amplitudes since $A_l\to 0$ for that range of l values. A quantitative demonstration of this fact is shown in Fig. 6. There, along with a plot of T_l determined from the Cu scattering data, we show $\sigma(\theta)/\sigma_R(\theta)$, the ratio to Rutherford scattering, calculated with $\delta_l=0$ for $l<l'$. With $l'=13$ or 14, only very minor changes are seen at the larger angles. Finally, when $l'=15$, for which $A_{l'}\cong 0.1\,(T_{l'}\cong 0.99)$, the angular distribution is severely distorted, again at the larger angles. This emphasizes the senstivity of the larger momentum-transfer scattering to the values of δ_l in the smaller orbital angular-momentum states, and it indicates that a more justifiable form of δ_l than that given in Eq. (3) could best be tested by precise large momentum-transfer scattering data. This would be true particularly in instances of weaker absorption, where A_l would not vanish for the smaller values of l.

III. CONCLUSIONS

In summary, PPS and CPM analyses of the elastic scattering of strongly absorbed particles are seen to be equivalent. Some advantages of the PPS treatment are the following:

(1) The calculation is simpler than for the CPM, since the numerical solution of Eq. (4) is by-passed. This is particularly advantageous whenever large numbers of partial waves contribute to the scattering.

(2) The form of $A_l(r)$ gives a clear physical interpretation of the absorption of the incident particles, and we believe that for strong-absorption scattering the determined $A_l(r)$ curve is essentially unique. On the other hand, the CPM varies the parameters of $V_N(r)$ to produce this $A_l(r)$ curve, and ambiguities in the potentials describing, for example, alpha-particle[13] and deuteron[14] scattering, result from the fact that different potentials can give essentially the same $A_l(r)$ and $\delta_l(r)$ values. Clearly the value of $V_N(r)$ for $r<r'$, where $A_l(r)=0$ for $r<r'$, can have no effect on the scattering.

(3) The PPS analysis described in this paper has found application in the calculation of inelastic scattering of alpha particles, through the model of Austern and Blair.[15] In this model the inelastic scattering amplitudes are expressed in terms of derivatives of the partial-wave amplitudes for elastic scattering, η_l. The equivalence between the Austern-Blair model and distorted-wave Born-approximation calculations for inelastic scattering is analogous to the equivalence of PPS and CPM analyses for elastic scattering. Points (1) and (2) mentioned above are equally valid in this case.[16]

(4) Equation (1) for the scattering amplitude is valid, also in the relativistic region insofar as spin effects are unimportant.

---

[13] G. Igo, Phys. Rev. Letters **1**, 72 (1958).
[14] C. M. Perey and F. G. Perey, Phys. Rev. **122**, 755 (1963); E. C. Halbert, Nucl. Phys. **50**, 353 (1964).
[15] N. Austern and J. S. Blair, Ann. Phys. (N. Y.) (to be published).
[16] J. Alster and D. C. Shreve, Bull. Am. Phys. Soc. **10**, 130 (1964); A. Springer and B. G. Harvey, Phys. Rev. Letters **14**, 316 (1965).

ACKNOWLEDGMENTS

For valuable discussion at various times, we are grateful to Dr. J. S. Blair, Dr. A. E. Glassgold, Dr. K. R. Greider, Dr. J. G. Vidal, Dr. D. S. Saxon, and Dr. M. A. Melkanoff. Doctor G. Igo was particularly helpful in making available the phase shifts from his complex-potential-model calculations. One of us (J.A.) wants to thank Dr. A. H. Wapstra for his interest in this work.

PHYSICAL REVIEW VOLUME 139, NUMBER 1B 12 JULY 1965

Density Effect on Energy versus Range of Fission Fragments in Gases*

C. B. FULMER
Oak Ridge National Laboratory, Oak Ridge, Tennessee
(Received 5 February 1965)

The density effect on specific energy loss of fission fragments in gases is discussed. Previously reported range-versus-energy data for median-mass light and heavy fission fragments in H_2, He, air, and Ar are corrected for saturation of the density effect.

IN a previously reported experiment,[1] fission fragments were degraded in energy by various stopping materials. Energies were measured as a function of thickness of stopping material traversed by the fragments. These data were used to obtain range-versus-energy curves for median-mass light and heavy fragments in the several materials. The materials included gases and metallic foils. The energies were determined by scintillation pulse-height measurements at the focal plane of a magnetic spectrograph.[2] The flight path from the fission foil to the focal plane was ~7.5 m. For the measurements with gases the system was filled with the gas being studied. The pressure varied up to a few Torr. For presentation of the data in Ref. 1, the 7.5-m path lengths in gas at low pressures were converted to equivalent thicknesses of gas at atmospheric pressure. The data as presented in Ref. 1 are not corrected for the density effect on the specific energy loss of the fission fragments,[3] and hence are valid only for pressures at which the data points were taken. The purpose of this note is to present the previously reported range-energy data for fission fragments in gases with corrections for saturation of the density effect.

The density effect on specific energy loss of fission fragments in gases is due to the variation of equilibrium charge Z_{av} with pressure at low gas pressures.[4] The density effect on Z_{av} was studied experimentally (Ref. 4) for light and heavy fission fragments in hydrogen, helium, air, and argon. The results of that

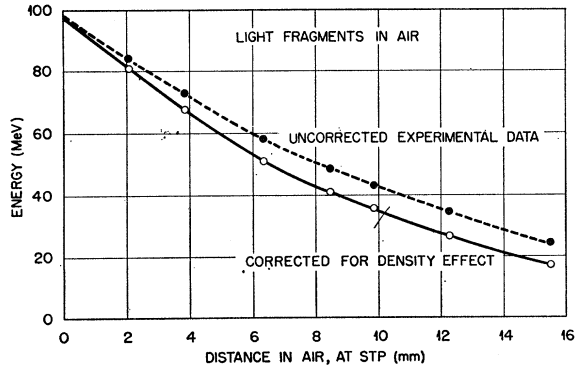

FIG. 1. Uncorrected and corrected data for light fragments in air.

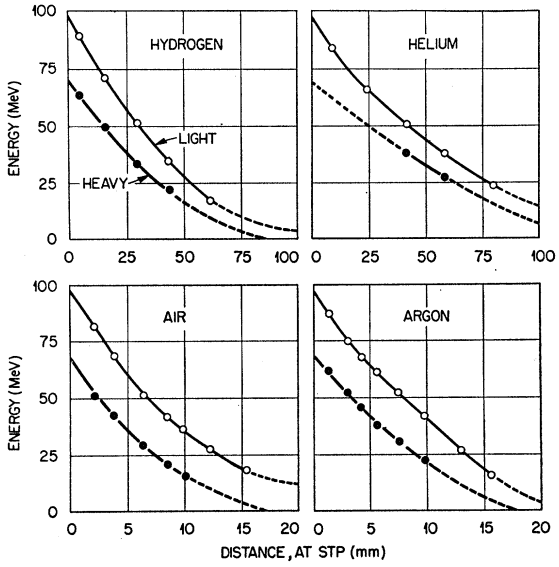

FIG. 2. Energy versus distance traveled for median-mass light and heavy fission fragments in gases. The data are corrected for saturation of the density effect.

* Research sponsored by the U. S. Atomic Energy Commission under contract with the Union Carbide Corporation.
[1] C. B. Fulmer, Phys. Rev. **108**, 1113 (1957).
[2] B. L. Cohen and C. B. Fulmer, Nucl. Phys. **6**, 547 (1958).
[3] Pablo Mulas and R. C. Axtmann (private communication).
[4] C. B. Fulmer and B. L. Cohen, Phys. Rev. **109**, 94 (1958).